Eukaryotic Ribosome Assembly

Arnaud Vanden Broeck and Sebastian Klinge

Laboratory of Protein and Nucleic Acid Chemistry, The Rockefeller University, New York, New York, USA; email: klinge@rockefeller.edu

Annu. Rev. Biochem. 2024. 93:189–210

First published as a Review in Advance on May 20, 2024

The *Annual Review of Biochemistry* is online at biochem.annualreviews.org

https://doi.org/10.1146/annurev-biochem-030222-113611

Keywords

ribosome biogenesis, ribosome assembly, eukaryotic ribosome, RNA folding, rRNA processing, cryo–electron microscopy

Abstract

During the last ten years, developments in cryo–electron microscopy have transformed our understanding of eukaryotic ribosome assembly. As a result, the field has advanced from a list of the vast array of ribosome assembly factors toward an emerging molecular movie in which individual frames are represented by structures of stable ribosome assembly intermediates with complementary biochemical and genetic data. In this review, we discuss the mechanisms driving the assembly of yeast and human small and large ribosomal subunits. A particular emphasis is placed on the most recent findings that illustrate key concepts of ribosome assembly, such as folding of preribosomal RNA, the enforced chronology of assembly, enzyme-mediated irreversible transitions, and proofreading of preribosomal particles.

Contents

INTRODUCTION

Functional Architecture of Ribosomal Subunits and Their Assembly

In all domains of life, protein synthesis is catalyzed by ribosomes, RNA–protein molecular machines whose biogenesis involves a vast ensemble of assembly factors (**Figure 1**). In eukaryotes, the 80S ribosome is composed of two subunits, with the small subunit (SSU; 40S) responsible for decoding of messenger RNA (mRNA) and the large subunit (LSU; 60S) responsible for peptide bond formation. Ribosomes are ribozymes, as the catalytic activity of both subunits (mRNA decoding and peptide bond formation) is catalyzed by ribosomal RNAs (rRNAs), which are stabilized by ribosomal proteins (1). The SSU rRNA (18S) is composed of four domains (5′, central, 3′ major, and 3′ minor) that are brought together through a universally conserved tertiary structure, the central pseudoknot. This arrangement gives rise to the characteristic architecture of the SSU with body and head domains, between which the decoding center (DC) interrogates mRNA–transfer RNA interactions (**Figure 1*b***).

The LSU rRNAs (25S/28S in yeast/humans, 5.8S, and 5S) adopt a more complex structure as the 25S/28S rRNA contains six domains (I–VI), of which domain I interacts extensively with the 5.8S rRNA. All six domains arise from root helices, which represent their origins and boundaries. In addition, these rRNA elements form several functional centers including the peptidyl transferase center (PTC), the L1 stalk, and the polypeptide exit tunnel (PET). The 5S rRNA is part of the central protuberance (CP), a key architectural element of the LSU (**Figure 1*b***).

The folding of these rRNA elements, which include the active centers (such as the DC for the SSU and PTC for the LSU) and key architectural elements (including the central pseudoknot and root helices), is chaperoned in a highly coordinated manner to guarantee a rapid and continuous supply of functional ribosomes.

The assembly of eukaryotic ribosomes involves the complex chaperoned folding of preribosomal RNAs (pre-rRNAs) by more than 200 transiently associated ribosome assembly factors, as well as ribosomal proteins that are permanent components of each mature ribosomal subunit. This pathway occurs in three subcellular compartments, the nucleolus, the nucleus, and the cytoplasm

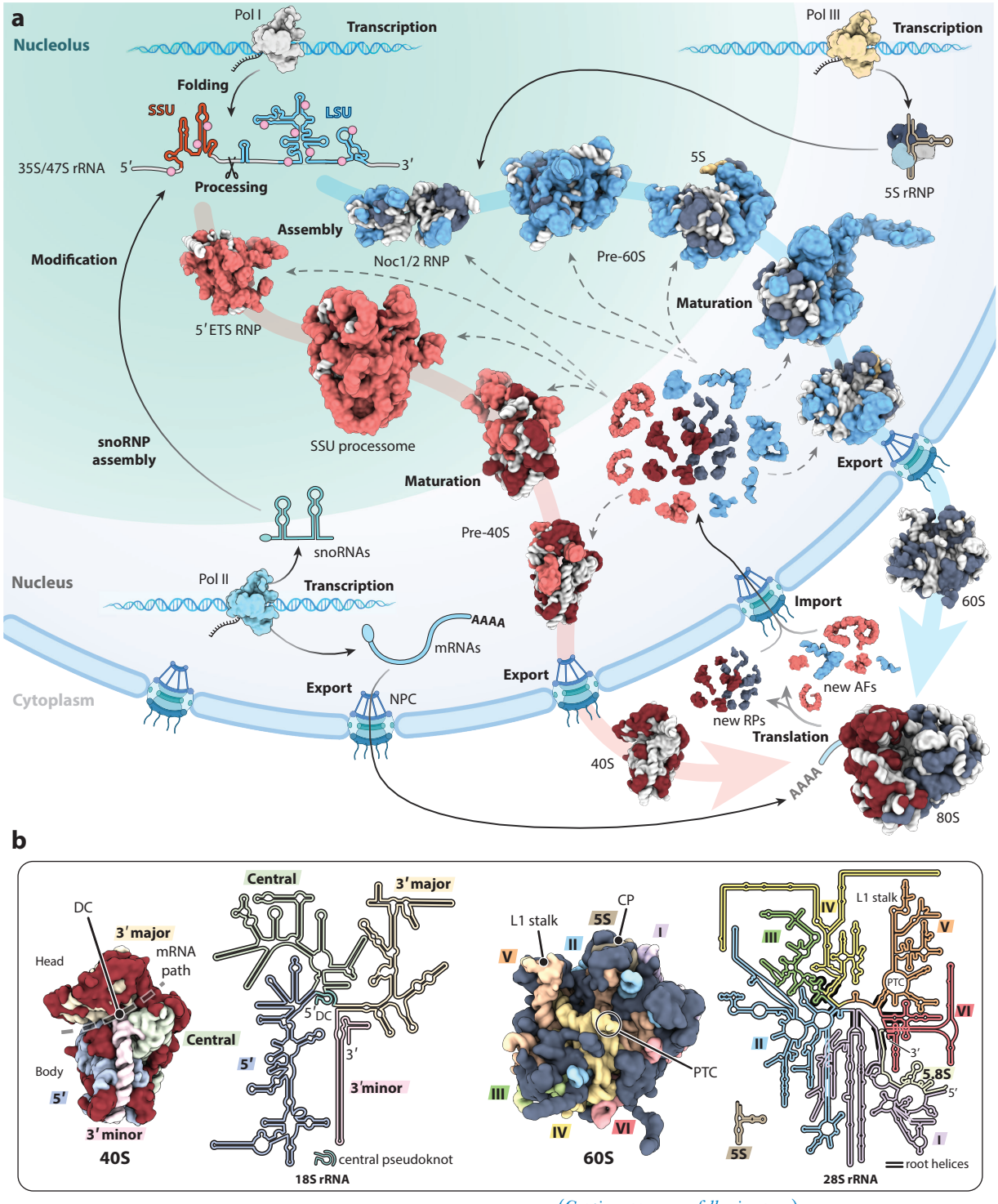

(*Caption appears on following page*)

Figure 1 (*Figure appears on preceding page*)

Assembly and functional architecture of eukaryotic ribosomal subunits. (*a*) Schematic overview of eukaryotic ribosome assembly with Pol I–mediated transcription of preribosomal RNA followed by initial folding, chemical modification, and processing. Early precursors of the small and large ribosomal subunits are assembled in the nucleolus, matured in the nucleus, and exported into the cytoplasm where the mature SSU (40S) and LSU (60S) join to form the 80S ribosome. Protein synthesis by 80S ribosomes generates new RPs and AFs, which are reimported into the nucleus and nucleolus to assemble new preribosomal particles. RNAs are color coded with segments originating from the long precursor species (35S/47S) in white, mRNAs and snoRNAs synthesized by Pol II in cyan, and 5S rRNA synthesized by Pol III in light brown. AFs and RPs are colored in light and dark shades, respectively, of red (SSU) and blue (LSU). (*b*) Functional architecture and rRNA secondary structures of human ribosomal subunits. Secondary structures are color coded by domain with structural elements for the SSU (central pseudoknot) and LSU (root helices) indicated. Functional centers of each subunit are shown in the corresponding 3D structure depictions. Abbreviations: AF, assembly factor; CP, central protuberance; DC, decoding center; ETS, external transcribed spacer; LSU, large subunit; mRNA, messenger RNA; NPC, nuclear pore complex; Pol, RNA polymerase; PTC, peptidyl transferase center; RP, ribosomal protein; rRNA, ribosomal RNA; RNP, ribonucleoprotein; rRNP, ribosomal RNP; snoRNA, small nucleolar RNA; snoRNP, small nucleolar RNP; SSU, small subunit.

(**Figure 1*a***). Within the nucleolus, RNA polymerase I initially synthesizes a large pre-rRNA (35S in yeast, 47S in humans) that contains the 18S rRNA and two of the three LSU rRNAs (25S and 5.8S in yeast, 28S and 5.8S in humans) flanked by external transcribed spacers (5′ ETS and 3′ ETS) and interspersed by internal transcribed spacers (ITS1 and ITS2). This precursor undergoes cotranscriptional folding, processing, and modification so that the assembly and initial maturation of both subunits occur within the nucleolus. This is followed by further maturation in the nucleus and nuclear export to enable the final stages of assembly and quality control in the cytoplasm (**Figure 1*a***; **Supplemental Figure 1**). Within the cytoplasm, newly formed 80S ribosomes then synthesize proteins including RNA polymerases, assembly factors, and ribosomal proteins that are imported back into the nucleolus/nucleus to sustain the continuous cycle of ribosome assembly.

Supplemental Material >

Technology-Driven Discoveries in Eukaryotic Ribosome Assembly

Since the discovery of ribosomes in 1955 (2), and the subsequent identification of pre-rRNA processing in human cells in the early 1960s (3, 4), our understanding of eukaryotic ribosome assembly has developed as new technologies have become available. Indeed, electron microscopy was transformative not only for the initial identification of ribosomes but also for the study of their cotranscriptional assembly on what subsequently became known as Miller spreads (5). While early functional studies predominantly focused on pre-rRNA processing (6), *Saccharomyces cerevisiae* quickly emerged as a powerful model system in which molecular genetics could be used to identify numerous assembly factors of both ribosomal subunits (reviewed in 7). The development of tandem affinity purifications and mass spectrometry (8, 9) subsequently led to the identification of many additional ribosome assembly factors that could now be studied biochemically as part of their native complexes (reviewed in 10). With the structure determination of mature ribosomal subunits in the early 2010s by X-ray crystallography (11–14), the products of eukaryotic ribosome assembly were revealed, for the first time providing a high-resolution structural perspective. The development of RNA–protein cross-linking methods (15) enabled RNA-binding sites of ribosome assembly factors to be mapped, thereby providing important foundations for subsequent biochemical and structural studies. Since 2016 the resolution revolution in cryo–electron microscopy (cryo-EM) (16) had a significant impact on the study of eukaryotic ribosome assembly, as native ribosome assembly intermediates could now be visualized at resolutions of approximately 3 Å for the first time (17). As a result of these developments, isolated structures of both LSU and SSU assembly intermediates could be obtained from yeast and human cells (reviewed in 18, 19).

During the last four years, significant progress has been made in several areas of eukaryotic ribosome assembly, which is the focus of this review. As a result, instead of providing a

comprehensive summary of all aspects of ribosome assembly, this review provides a current perspective on the most recent scientific developments. These include new insights into early cotranscriptional assembly intermediates, key nucleolar transitions, and early assembly events in human cells.

Key Themes of Eukaryotic Ribosome Assembly

Throughout this review, we highlight examples of the following recurring themes of eukaryotic ribosome assembly:

1. The most fundamental aspect of eukaryotic ribosome assembly is the folding of pre-rRNA, during which the conformational freedom of pre-rRNA is systematically reduced as a function of time. This is primarily achieved through the transient stabilization of correctly folded pre-rRNA elements by ribosome assembly factors and the stabilization of more mature rRNA folding states by ribosomal proteins.
2. The chronology of ribosome assembly is essential and follows several rules to ensure that ribosome assembly factors associate and dissociate from preribosomal assembly intermediates at the right time. Co- and posttranscriptional tethering of ribosome assembly factor complexes ensures that assembly factors required for later stages of assembly are already associated with their substrate particles. Here, tethering may determine the order in which different assembly factors occupy a given binding site, especially if binding of different assembly factors is mutually exclusive or if molecular mimicry is employed. As a function of pre-rRNA folding, large-scale conformational changes of pre-rRNA can be used to abolish old binding sites for assembly factors and generate new ones, thereby dictating the chronology of association. While many aspects of eukaryotic ribosome assembly follow hierarchical patterns, parallel processing of different assembly events is also observed. In these instances, parallel processing may provide benefits as it enables several events to occur simultaneously, thereby increasing the overall efficiency of ribosome assembly without affecting its fidelity.
3. Irreversible steps during eukaryotic ribosome assembly are used in conjunction with assembly checkpoints. These irreversible steps may require molecular switches in the form of nucleotide hydrolyzing enzymes (ATPases or GTPases) that mediate pre-rRNA folding transitions. Endonucleolytic cleavages can be used to irreversibly separate pre-rRNA molecules, while exonucleolytic removal of pre-rRNA can be employed to bring about conformational as well as compositional changes in a given precursor. Similarly, large AAA-ATPases are employed to irreversibly remove assembly factors from maturing particles.
4. Structural and functional proofreading of functional centers of preribosomal particles is accomplished by assembly factors that continuously interrogate and proofread the correct assembly status of these pre-rRNA regions and their surrounding protein elements.

NUCLEOLAR ASSEMBLY AND RIBOSOMAL RNA MATURATION

Eukaryotic ribosome assembly is initiated in the nucleolus, a substructure of the nucleus, which in higher eukaryotes is further subdivided into three subcompartments: the fibrillar center (FC), the dense fibrillar component (DFC), and the granular component (GC) (20–22). The formation and maintenance of the nucleolus depend on active transcription of ribosomal DNA repeats by RNA polymerase I and associated regulatory factors that are located within the FC (23–26). Transcription of ribosomal DNA by RNA polymerase I enables cotranscriptional ribosome assembly events by providing pre-rRNA as a landing platform for early ribosome assembly factors located in the DFC. The GC contains maturing preribosomal particles of both subunits.

Both co- and posttranscriptional pre-rRNA processing have been observed, and while the majority of pre-rRNA processing in *S. cerevisiae* occurs cotranscriptionally (27), most pre-rRNA processing in human cells occurs posttranscriptionally (28). Following the earliest evidence of posttranscriptional pre-rRNA processing (3, 4), subsequent work from the 1970s (6, 29) identified a pre-rRNA species (then termed 37S) containing the RNA segments of both ribosomal subunits, which was associated with 90S particles. Separately, cotranscriptional ribosome assembly was first visualized in the late 1960s on Miller spreads, where the emergence of characteristic terminal balls represents the formation of small and large ribosomal subunit precursors (5).

Chemical modifications of pre-rRNA occur both co- and posttranscriptionally in eukaryotes. While a small number of assembly factors can directly catalyze chemical modifications of pre-rRNA, most covalent modifications of eukaryotic pre-rRNAs are catalyzed by two classes of small nucleolar ribonucleoprotein particles (snoRNPs) (30–32) (**Figure 1*a***). One class of these snoRNPs (Box C/D snoRNPs) consists of architectural proteins Nop56, Nop58, and Snu13 and a Box C/D snoRNA to guide the methyltransferase Nop1 for 2′-*O*-ribose methylation of pre-rRNA. The second class (H/ACA snoRNPs) consists of architectural proteins Gar1, Nop10, and Nhp2 together with box H/ACA snoRNAs that guide the pseudouridine synthase Cbf5 toward its pre-rRNA substrates. By base pairing with pre-rRNA sequences surrounding the nucleotide that is modified, snoRNAs also act as RNA chaperones. Other snoRNAs also perform numerous additional functions during pre-rRNA processing beyond guiding chemical modifications of pre-rRNA, such as U3 snoRNA and snR190, which act as purely structural RNA chaperones of SSU and LSU pre-rRNAs as discussed below, or RNase MRP, which catalyzes the posttranscriptional separation of small and large ribosomal subunit pre-rRNAs (33).

Beyond pre-rRNA modifications, many additional enzymes catalyze irreversible steps during ribosome assembly. These include ribonucleases (reviewed in 34, 35) and RNA-remodeling enzymes, such as 19 RNA helicases that are members of two distinct classes of enzymes, the DEAD-box and DEAH-box families. While some RNA helicases have been implicated in the assembly of both ribosomal subunits (DEAD-box helicase Has1, DEAH-box helicase Prp43, and the RNA exosome–associated Ski2-like helicase Mtr4), others are dedicated to either SSU assembly (DEAD-box helicases Dbp4, Dbp8, Fal1, Rok1, and Rrp3 and DEAH-box helicases Dhr1 and Dhr2) or LSU assembly (DEAD-box helicases Dbp2, Dbp3, Dbp6, Dbp7, Dbp9, Dbp10, Drs1, Mak5, and Spb4) (reviewed in 36–39). Molecular switches in the form of ATPases (Rio1, Rio2, and Fap7), processive AAA-ATPases (Mdn1, Rix7, and Drg1) (reviewed in 40), and GTPases (Bms1, Nog1, Nug1, Nog2, Lsg1, and Efl1) are used to catalyze unidirectional steps by combining nucleotide hydrolysis with RNA conformational changes or removal of protein components from maturing preribosomal particles. However, most ribosome assembly factors lack enzymatic activities and instead act as chaperones, either of the rRNA, by stabilizing specific pre-rRNA transition states, or of ribosomal proteins before these are integrated into preribosomal particles (41–43; reviewed in 44).

ASSEMBLY OF THE RIBOSOMAL SMALL SUBUNIT

Small Subunit Processome Formation

The initial identification of the terminal ball structures on Miller spreads as maturing pre-rRNAs of both subunits (5) was followed by later studies that identified one set of these particles as pre-rRNA processing assemblies containing the 5′ ETS, 18S rRNA, and the RNA chaperone U3 in *Xenopus laevis* (45, 46). The identification and biochemical characterization of the *S. cerevisiae* SSU processome as a large RNA–protein complex containing pre-rRNA (5′ ETS–18S) and U3 snoRNA–associated proteins provided an important inroad toward its subsequent mechanistic

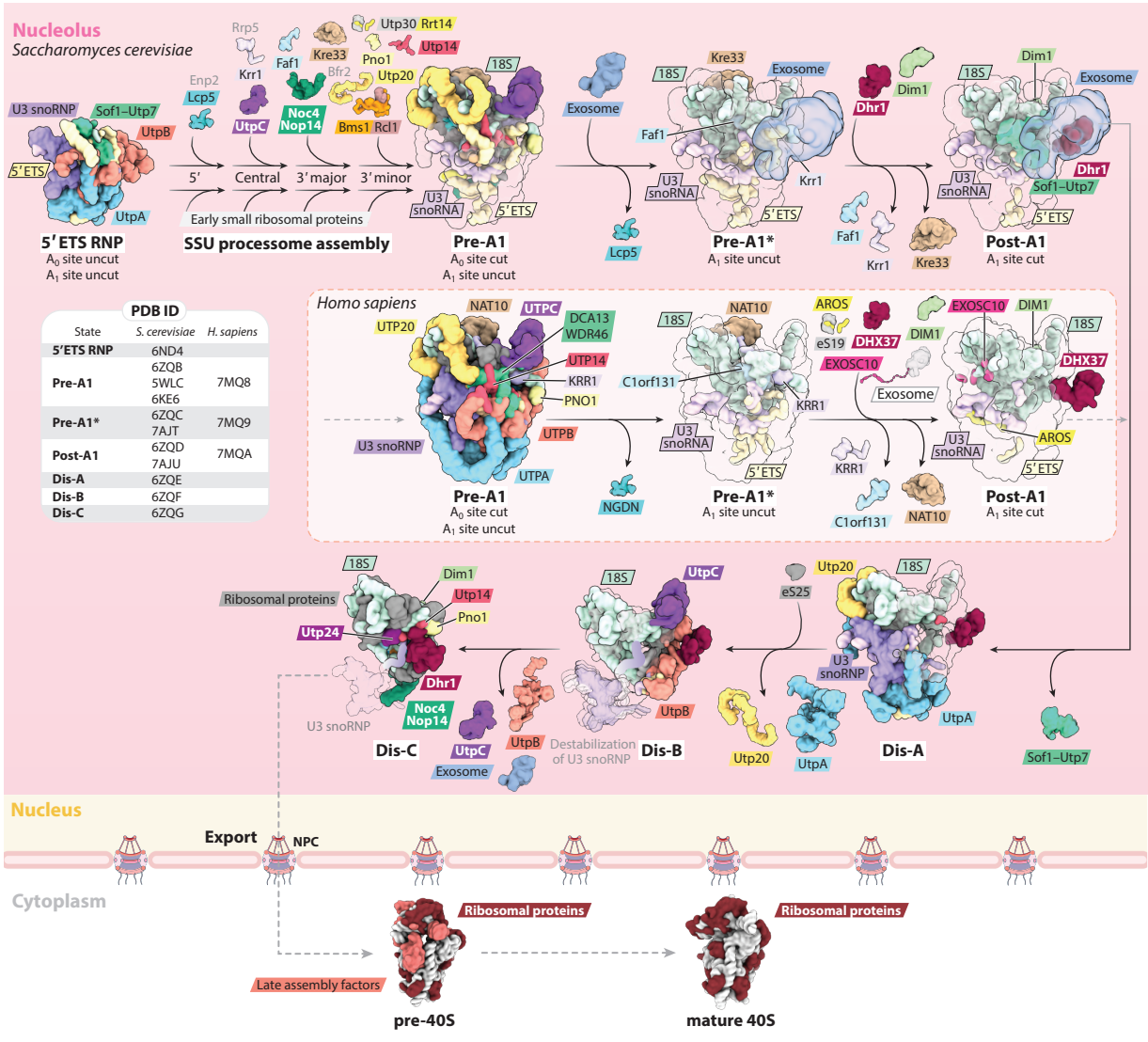

Figure 2

Maturation of the eukaryotic small ribosomal subunit in *Saccharomyces cerevisiae* and humans. Schematic depiction of nucleolar assembly of the SSU processome from a 5′ ETS RNP, followed by maturation of the SSU processome through three stages (pre-A1, pre-A1*, and post-A1) during which the 5′ ETS is eliminated by the RNA exosome. Nucleolar maturation of late SSU processome disassembly intermediates and cytoplasmic maturation are shown for yeast only. Protein complexes equivalent between the yeast and human systems are color coded accordingly, and the human states are shown within the light-pink box. Arrows indicate the progression of intermediates as well as the arrival and departure of assembly factors. PDB IDs representing equivalent structures are indicated. Abbreviations: ETS, external transcribed spacer; NPC, nuclear pore complex; PDB ID, Protein Data Bank identifier; RNP, ribonucleoprotein; snoRNP, small nucleolar RNP; SSU, small subunit.

characterization (47) (**Figure 2**). The isolation of a similar particle containing SSU assembly factors but lacking LSU assembly factors was initially thought to represent the 90S particle, as the presence of the 5′ ETS was believed to indicate the presence of a 35S pre-rRNA species (48, 49). However, since all biochemical and structural data from yeast and human cells show that both

particles are indeed SSU processomes, which lack 35S pre-rRNA and LSU assembly factors (50–57), we refer to this particle as the SSU processome. Our current mechanistic understanding of SSU processome formation is based on biochemical studies of associated multi-protein complexes (58–61), the effects of protein depletion experiments (62, 63), experiments involving truncation of the 5′ ETS (64), and the use of pre-rRNA mimics tagged with RNA aptamers that highlighted assembly factor association as a function of transcription (65, 66). Importantly, the 5′ ETS and all subdomains of the 18S rRNA can each independently recruit their own set of assembly factors prior to a compaction step that requires the presence of all domains. In this compaction step, early domain-specific chaperones are evicted while proteins on the periphery of the mature SSU processome and processing factors, such as the RNA exosome and the DEAH-box helicase Dhr1, are stabilized (67) (**Figure 2**). At the beginning of pre-rRNA synthesis, the 5′ ETS RNP is formed, a 2-MDa particle that contains the 5′ ETS, U3 snoRNA, and early assembly factors. The structure of the 5′ ETS RNP highlights the fact that large-scale conformational switches of nascent preribosomal particles can be used to control the availability of binding sites, thereby determining the chronology of early assembly. Within the 5′ ETS RNP, the 5′ ETS is already chaperoned by several assembly factor complexes, such as UtpA, UtpB, and the U3 snoRNP, of which U3 snoRNA base pairs with the 5′ ETS via its 3′ and 5′ hinges (61, 67) (**Figure 2**). While we currently lack structural information on how the four subdomains of the 18S rRNA (5′, central, 3′ major, and 3′ minor) are transiently chaperoned by early assembly factors, structures of fully formed SSU processomes have provided us with a clear picture showing that these domains are housed in different regions of this particle (50–57). Within the SSU processome, U3 snoRNA performs a central function by preventing the premature formation of the central pseudoknot by base pairing with parts of the 18S rRNA that form this structure in the mature 40S subunit.

Small Subunit Processome Maturation Toward a 40S Subunit

More recently, we have obtained the first insights into how the RNA exosome participates in the maturation of yeast and human SSU processomes to trigger cleavage at site A1 by the endonuclease Utp24, thus separating the 5′ ETS from the 18S rRNA (55–57, 68–70). All currently available structural data highlight that the RNA exosome is tethered to the SSU processome via flexible peptides (57, 71), which explains why featureful cryo-EM maps of RNA exosome components associated with the SSU processome are lacking. Whereas the precise role of the RNA exosome in SSU processome maturation was initially unclear (55, 56, 70), higher-resolution data on maturing human SSU processomes allowed a first model for exosome-driven and Utp24-mediated A1 cleavage to be proposed (57, 72). Key to this model is that the 5′ ETS is unwound as a function of exosome activity, resulting in the dissociation of assembly factors, while also allowing the entire SSU processome to undergo large-scale conformational changes that are subsequently read out by peptide-like assembly factors such as Utp14, among others (72) (**Figure 2**). However, how these steps are organized at a mechanistic level remains poorly understood.

In addition to providing a structural context for diseases that are associated with mutations in human ribosome assembly factors and ribosomal proteins, the human SSU processome further illustrates the degree to which evolution has allowed for expansion of this structure. While the size of the human 5′ ETS is approximately five times larger than its yeast counterpart, functional studies have shown that most of the expanded segments are dispensable for ribosome assembly and project into the solvent (57). Following the processing of the 5′ ETS by the RNA exosome (the post-A1 state), the DEAH-box RNA helicase Dhr1/DHX37 docks on yeast and human SSU processomes and is subject to further repositioning on the surface of the particle (**Figure 2**). Several states of Dhr1 have been described, with the first crystal structures of yeast and mouse Dhr1

determined in the apo and RNA-bound states, respectively (73, 74). While a cryo-EM structure of yeast Dhr1 bound to the SSU processome was initially interpreted as an ADP-bound off state (55), the crystal structure of an autoinhibited ADP-bound state of yeast Dhr1 showed how Dhr1 can be recruited to the SSU processome in an inactive state (57).

During subsequent stages of SSU processome maturation, Dhr1 unwinds U3 snoRNA from the SSU processome (55, 75–77), yet how Dhr1 is released from its autoinhibited state remains unclear. In addition, the functional interplay and timing between the actions of the DEAH-box helicase Dhr1, Utp14, the GTPase Bms1, and the methyltransferase Bud23, which has been well characterized genetically (78), remain to be elucidated mechanistically. Late nuclear and cytoplasmic states of pre-40S particles are characterized by a gradual formation of the head region and final trimming of the 18S rRNA (79–83), processes that have recently been reviewed (19, 72).

ASSEMBLY OF THE RIBOSOMAL LARGE SUBUNIT

Cotranscriptional Assembly in the Nucleolus

The cotranscriptional assembly of the large ribosomal subunit occurs immediately following the transcription of the SSU pre-rRNA and shares a common theme with SSU assembly: A precursor segment (5′ ETS for the SSU, ITS2 for the LSU) serves as a landing platform for ribosome assembly factors that organize subsequent assembly events. However, in contrast to the SSU rRNA, there are six domains (I–VI) in the LSU rRNA (25S in yeast, 28S in humans), with root helices forming the bases for these domains. In addition, cotranscriptional LSU assembly is organized such that the 5.8S rRNA, ITS2, and domains I and II of the 25S/28S rRNA act as an initial recruitment platform for assembly factors, and it is only upon complete transcription of the entire LSU transcript that the association of many additional assembly factors is observed (84, 85) (**Figure 3**). The first cotranscriptional LSU assembly intermediate for which we have structural information (Noc1–Noc2 RNP) highlights key concepts of ribosome assembly: Assembly factors such as the Noc1–Noc2 complex stabilize correctly folded root helices of domains I and II as well as the 5′ end of the pre-rRNA. In addition, the binding of the Noc1–Noc2 complex facilitates the association of both ribosomal proteins and other assembly factors (86). On the solvent-exposed side of the nascent pre-60S, the iron–sulfur cluster–containing assembly factor Mak16 has a key role by recruiting Rpf1 and Nsa1 (WDR74 in humans), which later stabilize the solvent-exposed side near the forming PET in State 2 (yeast) and its equivalent State A (human) (**Figure 3**). Similarly, domains V and VI are chaperoned by snR190 and stabilized by structural assembly factors including the Urb complex (Urb1, Urb2, Rsa3, and Nop8) (87–89), while several DEAD-box RNA helicases (Dbp6, Dbp7, and Dbp9) participate in remodeling and incorporating domains V and VI into the early pre-60S particle, which juxtaposes the 5′ and 3′ regions of the 25S/28S rRNA, as observed in State 2 (yeast) and State A (human) (90–93) (**Figure 3**). With both the 5′ and 3′ ends now processed, the solvent-accessible surface of the LSU is formed first, so that the incorporation of domains V, III, and IV can occur during nucleolar posttranscriptional assembly (94–96). At the center of State 2 is a heterotrimeric complex (Ssf1–Rrp15–Rrp14), which stabilizes the interface between domains II and VI while also organizing the root helices of domains III–V (**Figure 3**).

Posttranscriptional Assembly in the Nucleolus

With the formation of State 2 (human State A), nucleolar posttranscriptional assembly of the large ribosomal subunit proceeds, and functional centers of the LSU, including the PET, the L1 stalk, and the PTC, are assembled. During the past 6 years, structures of nucleolar pre-60S assembly intermediates have been obtained from yeast and human cells, providing both overarching principles as well as species-specific adaptations of this process (17, 94–106). Here we discuss nucleolar pre-60S particles from *S. cerevisiae* (Noc1–Noc2 RNP, States 2, C, E1, E2, NE1, NE2, and Nog2)

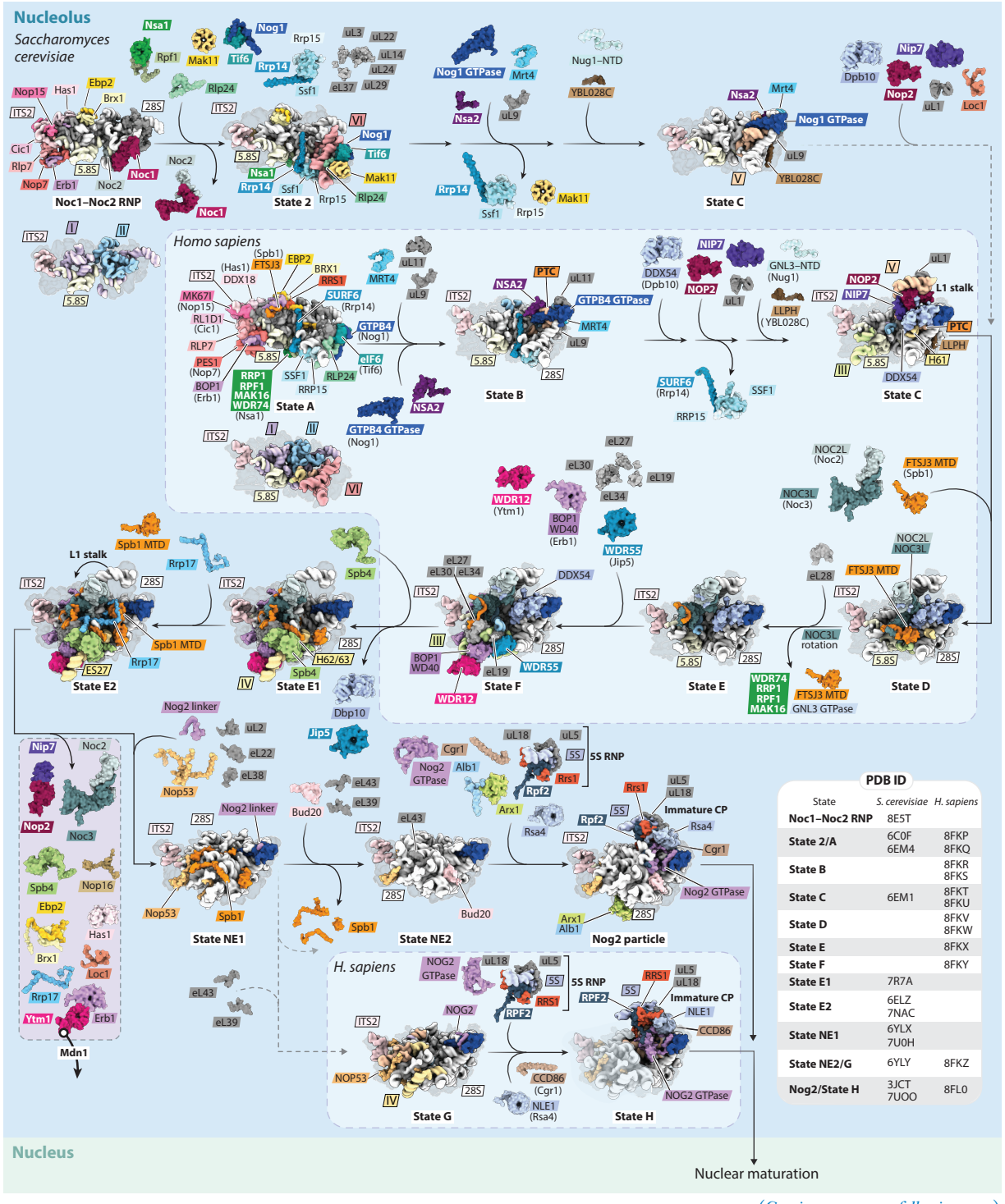

(Caption appears on following page)

Figure 3 (*Figure appears on preceding page*)

Nucleolar assembly of the large ribosomal subunit in *Saccharomyces cerevisiae* and humans. Schematic depiction of *S. cerevisiae* nucleolar assembly with the equivalent human steps shown in the light-blue boxes. The rRNA domains (ITS2; domains I, II, and VI; and 5.8S) are shown separately for cotranscriptional (*S. cerevisiae* Noc1–Noc2 RNP) and posttranscriptional assembly intermediates (human State A), with equivalent domains colored identically. Arrows highlight transitions and the association or dissociation of protein components. Equivalent proteins are colored identically, and in cases where protein names are different, human proteins have the corresponding yeast name listed in parentheses. The table lists the names of states with corresponding PDB IDs that represent equivalent structures. The purple shaded box contains the network of early assembly factors removed by Mdn1. Abbreviations: CP, central protuberance; ITS, internal transcribed spacer; PDB ID, Protein Data Bank identifier; PTC, peptidyl transferase center; RNP, ribonucleoprotein; rRNA, ribosomal RNA.

and human cells (States A–H). Ribosome assembly factors are listed as named in the described species, and the names of corresponding assembly factors from the other species are indicated in parentheses (**Figure 3**).

An emerging theme is the use of parallel processing at the solvent-exposed side of early nucleolar pre-60S particles, where the early stages of LSU assembly (human States A–D) can proceed in either the presence or absence of a cluster of interacting proteins including Mak16, Rpf1, Nsa1, Rrp1, and Nug1 (human MAK16, RPF1, WDR74, RRP1, and GNL3) (106). The AAA-ATPase Rix7 (human NVL2) has been shown to remove this cluster from Nsa1 (human WDR74)-containing particles (107–109). However, since Nsa1 is missing in the thermophilic yeast *Chaetomium thermophilum* (104), the conserved removal of this complex is likely coordinated via the Mak16–Rpf1 heterodimer.

Following the incorporation of domain VI in State 2, elements of the PTC are installed by two energy-consuming enzymes, the GTPase Nog1 (human GTPB4) and the DEAD-box RNA helicase Dbp10 (human DDX54) (**Figure 3**). In human pre-60S structures, GTPB4 appears in a postcatalytic (GDP-bound) state with the first elements of the PTC (domain V) in State B. Subsequently, in State C, a second set of PTC elements is installed by DDX54, which also appears in a postcatalytic (ADP-bound) state, which remodels an extended root helix of domain IV (helix 61) and stabilizes the L1 stalk positioned in an immature state (106). By remodeling the root helix of domain IV, DDX54 is thought to release the SSF1–RRP15–SURF6 (yeast Ssf1–Rrp15–Rrp14) complex, thereby allowing for an irreversible partial compaction of the structure. Separately, DDX54 also recruits the NOC2L–NOC3L–FTSJ3 complex (yeast Noc2–Noc3–Spb1), which initially adopts a downward orientation in State D that facilitates the stabilization of parts of domain III. Intriguingly, the NVL2 (yeast Rix7)-mediated removal of the MAK16-associated complex is associated with a conformational change of the NOC2L–NOC3L–FTSJ3 complex in State E, which now permits the incorporation of domain III in State F (**Figure 3**). While the functional coupling underlying these events is currently unknown, an interplay between domain III–associated factors, NVL2, and the MAK16-associated cluster would explain this phenomenon.

The incorporation of domains III and IV is highly organized, with the earliest of these states from human pre-60S particles showing that WDR55 (yeast Jip5) initially chaperones domain III while also preventing the integration of parts of domain IV in State F (106). Studies in *S. cerevisiae* have shown that the DEAD-box RNA helicase Spb4 binds to domain IV in States E1 and E2 (**Figure 3**), remodeling rRNA helices 62/63 and thereby continuing remodeling close to sites that were previously remodeled by Dbp10 (human DDX54) (94, 95, 99, 105, 110). A recurring theme here is that Spb4 appears in a posthydrolysis (apo or ADP-bound) state (99, 105), showing that enzyme-catalyzed events in ribosome assembly overcome energetic barriers and therefore favor unidirectional progression. Assembly intermediates containing Spb4 also contain the Spb1 methyltransferase domain close to its substrate nucleotide in the A loop (G2922 in *S. cerevisiae*)

and can include the RNA chaperone Puf6, which was previously mapped to bind domain IV (RNA helices 68 and 69) in the context of pre-60S intermediates (84, 85, 104, 111).

In a subsequent step, the AAA-ATPase Mdn1 catalyzes the irreversible restructuring of the nucleolar pre-60S particle, bringing about large compositional and conformational changes (98, 112, 113) (**Figure 3**). While the requirements for and mechanism of this remodeling reaction of Mdn1 and the Rix1 subcomplex (yeast Rix1, Ipi1, and Ipi3; human PELP1, TEX10, and WDR18) (114) still remain unclear despite recent in vitro reconstitution experiments (105), the main consequence of this activity is the removal of early nucleolar assembly factors that are interconnected with the main substrate of Mdn1 (Ytm1–Erb1, human WDR12–BOP1), as shown in both yeast and human systems (94–96, 99, 105, 106). The removal of all assembly factors that are part of the Erb1–Ytm1-associated network (yeast Has1, Brx1–Ebp2, Noc2–Noc3, Nop2–Nip7, and Spb4; human DDX18, BRX1–EBP2, NOC2L–NOC3L, NOP2–NIP7, and DDX55) triggers large-scale rRNA conformational changes by releasing the L1 stalk from its immature position while also allowing interdomain rRNA–rRNA contacts to be formed. In addition to the removal of early assembly factors, a key compositional change involves the installation of Nop53, which not only blocks reassociation of earlier assembly factors that have mutually exclusive binding sites but is also a critical component for the removal of ITS2 during nuclear maturation (**Figure 3**). Subsequently the integration of the 5S RNP (5S rRNA, ribosomal proteins uL18 and uL5, and assembly factors Rpf2 and Rrs1) is achieved with contributions from rRNA and protein elements. Early biochemical data in *S. cerevisiae* already showed that 5S rRNA is part of pre-60S particles once domain VI is transcribed (84, 85), an interaction that is initially likely mediated by flexible RNA and protein components. This was recently confirmed at a structural level in multiple species, showing that extensions of Rrs1 and Rpf2 are assisting in the installation of the 5S RNP (104, 106, 115). These events result in the formation of a late nucleolar/early nuclear pre-60S assembly intermediate that contains the GTPase Nog2 and an immature CP with a rotated 5S RNP and associated chaperones Rpf2 and Rrs1 (17) (yeast Nog2 particle, human State H) (**Figure 3**).

Nuclear Maturation of pre-60S Particles

Biochemical and structural studies have shown that the 2′-*O*-methylation of G2922 by Spb1 affects the activity of Nog2, suggesting a precise interplay between an rRNA modification and Nog2 GTPase activity (100, 101). In a subsequent state, the AAA-ATPase Mdn1 is once again involved in a major remodeling step of the pre-60S particle and is observed following the rotation of the 5S RNP (17, 98, 112, 113, 116). The rotation of the 5S RNP involves many different assembly factors, including the 5S rRNA chaperones Rpf2 and Rrs1, which are removed in the process. Other involved assembly factors include general stabilizers such as Rsa4 and Cgr1 (human NLE1 and CCD86) as well as Mdn1-associated factors (**Figure 4**) (106, 117).

Intriguingly, under regular growth conditions, it is only upon 5S RNP rotation that ITS2 is processed, since Rpf2–Rrs1-containing particles (immature CP with 5S RNP unrotated) still contain ITS2 (17), whereas Mdn1-bound particles (mature CP with 5S RNP rotated) show signs of ITS2 processing (98). Due to the coupling of 5S RNP rotation with ITS2 processing, mutations in assembly factors involved in 5S RNP rotation result in the same RNA processing defects as mutations in assembly factors involved in ITS2 processing (115, 118–120). Recent structural data from human pre-60S particles suggest that there is a universal mechanism for this coupling. The departure of Rrs1 and Rpf2 during 5S RNP rotation, as well as the stabilization of the rotated 5S RNP by several Mdn1-associated assembly factors (yeast Sda1, Rix1, Ipi1, Ipi3, and Cgr1; human SDA1, TEX10, PELP1, WDR18, and CCD86), facilitates the accommodation of the L1 stalk in a bent conformation. It is this bent conformation of the L1 stalk that allows the N terminus of Nop53 to productively place the exosome close to the pre-60S particle (106). The positioning of

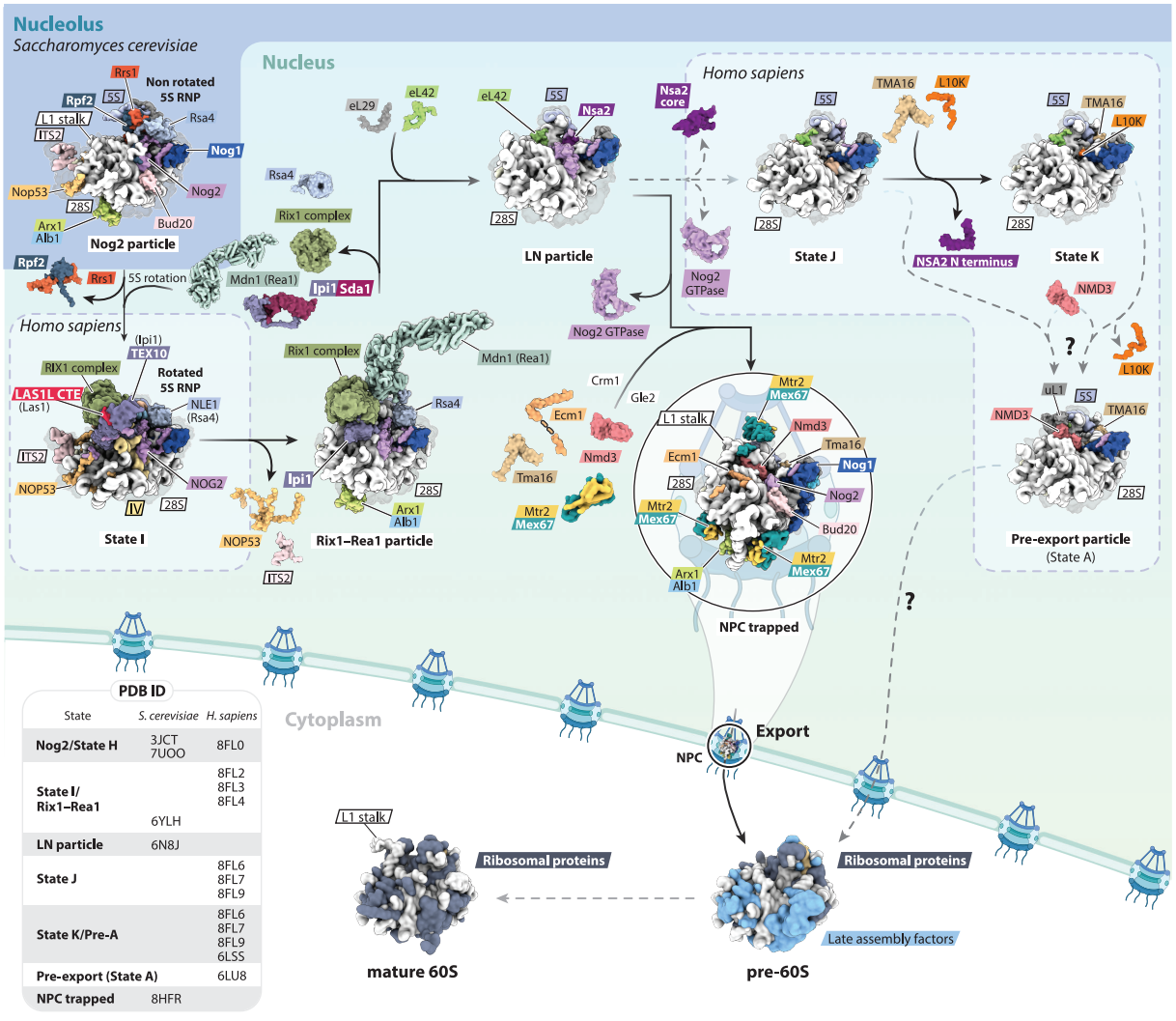

Figure 4

Nuclear maturation of the large ribosomal subunit in *Saccharomyces cerevisiae* and humans. Schematic depiction of *S. cerevisiae* nuclear maturation and export with the equivalent human pre-60S particles shown in the light-blue boxes. Arrows highlight transitions and the association or dissociation of protein components, with dashed arrows indicating more uncertain transitions. Equivalent proteins are colored identically, and in cases where protein names are different, human proteins have the corresponding yeast name listed in parentheses. The table lists names of states with corresponding PDB IDs that represent equivalent structures. Abbreviations: ITS, internal transcribed spacer; NPC, nuclear pore complex; PDB ID, Protein Data Bank identifier; RNP, ribonucleoprotein.

the exosome is further facilitated via an arch-interacting motif within Nop53 that interacts with the exosome-associated RNA helicase Mtr4 (71). While in human pre-60S particles the ITS2 endonuclease LAS1L (yeast Las1) and polynucleotide kinase NOL9 (yeast Grc3) are already docked (106, 114, 121), it is currently unclear how these enzymes are recruited to yeast pre-60S particles (**Figure 4**).

To functionally investigate ITS2 processing, in vitro reconstitution experiments and structural studies have been performed using Nop53-containing yeast pre-60S particles (122, 123). However,

given the coupled nature of 5S RNP rotation and ITS2 removal in vivo, the physiological relevance of in vitro ITS2 processing remains unclear, as under these conditions, particles also undergo ITS2 processing in the absence of 5S RNP rotation.

While the processing of ITS2 can be visualized in discrete steps in human cells (106), it remains unclear what triggers Mdn1 and associated assembly factors to dissociate and leave behind an export-competent pre-60S particle.

Nuclear Export and Cytoplasmic Maturation of Pre-60S Particles

Structures of yeast late pre-60S particles before and after nuclear export (124, 125) have very recently been complemented by the structure of a yeast pre-60S particle isolated from within nuclear pore complexes (NPCs) (**Figure 4**) (103). Collectively, these data now provide a first model of how nuclear export is achieved. The ability to adopt particular rRNA conformations is probed once again during nuclear export, when the L1 stalk is bent and stabilized by export factors in a way that is mutually exclusive with previously observed Mdn1-associated assembly factors (98). The central role of the bent L1 stalk further supports prior data showing that the L1 stalk is required for nuclear export (126). In addition, the presence of several export factors, including Gle2, Ecm1, Crm1, and three copies of Mex67–Mtr2, further suggests that multiple redundant binding events can catalyze nuclear export (**Figure 4**). In the center of the NPC-trapped pre-60S, both Nog2 and the export factor Nmd3 bind, possibly enabling a gradual replacement of Nog2 by Nmd3. In addition, the NPC-trapped pre-60S structure highlights that the binding sites of nuclear export factors do not require the removal of ITS2, rationalizing how ITS2-containing pre-60S particles can still be exported into the cytoplasm in yeast and human cells if ITS2 processing is compromised (106, 127, 128). Following nuclear export, the final stages of pre-60S biogenesis occur in the cytoplasm. Here, several states have been visualized that highlight the final formation of the peptidyl transferase center, the incorporation of the last ribosomal proteins, and the removal of the assembly factor RLP24 by the AAA-ATPase Drg1 (102, 124, 125, 129, 130).

HUMAN RIBOSOME ASSEMBLY AND DISEASE

Defects in eukaryotic ribosome assembly underline its central role at many different levels. They link compromised ribosome assembly with changes in nucleolar architecture, changes in cellular signaling with cancer, and changes in gene expression with the perturbed development of tissues. At a subcellular level, reduced levels of either ribosomal proteins or ribosome assembly factors result in changes to the nucleolar architecture (131–133). Within the nucleolus, changes in the levels of free 5S RNP are further coupled to altered p53 signaling, so patients suffering from ribosomopathies—human diseases in which ribosome assembly is compromised—also have an increased cancer predisposition (134). At the tissue level, reduced levels of ribosomal proteins decrease the overall pool of available ribosomes. This impacts the translation of rare transcripts, such as a transcription factor required for hematopoiesis (GATA1) whose absence results in anemia (135, 136). The molecular underpinnings of several ribosomopathies keep being identified (137, 138). Recent additions to this expanding list include mutations in ribosomal proteins (uL6 and uL2) (139, 140), assembly factors such as c1orf131 in the SSU processome (D. Lafontaine, personal communication), chaperones of ribosomal proteins such as HEATR3 (141, 142), and the RNA component of RNase MRP (143). To provide structural context for how mutations in human ribosomal proteins and assembly factors may affect ribosome assembly, new genome editing and biochemical approaches have been developed (57, 144, 145), which have allowed both very early assembly intermediates and mature forms of both human ribosomal subunits to be isolated for structural characterization (57, 106, 146–148). These structures, together with the identified

mutations, now provide a framework to better understand the molecular foundations of human ribosome assembly in health and disease.

OUTLOOK AND CONCLUSIONS

During the last decade, technological advances in cryo-EM have shifted our understanding of eukaryotic ribosome assembly from a list of protein names toward a molecular movie in which static frames are represented by individual high-resolution cryo-EM reconstructions of stable assembly intermediates. While providing a transformational change to the field, these advances now raise many new questions that likely require a set of new technologies and approaches. We currently lack a mechanistic understanding of how transitions between observed stable assembly intermediates are catalyzed. Similarly, there is an absence of both structural and mechanistic insights into the earliest events during the cotranscriptional assembly of both ribosomal subunits. Here, single-molecule approaches that have been essential for our understanding of fundamental principles of bacterial ribosome assembly may provide a promising avenue to fill these gaps (149, 150). Beyond ribosome assembly resulting in functioning ribosomes, the turnover of preribosomal components has recently come into focus (151, 152), raising new questions regarding how misassembled preribosomal particles are detected and subsequently degraded at the appropriate time and place. At the cellular level, we are faced with several orders of magnitude of scale to reach from the Ångstrom-level information observed in cryo-EM reconstructions of preribosomal particles to the micrometer scale of the human nucleus. Here, recent advances in cryo–electron tomography provide the means to contextualize both preribosomal particles and mature ribosomes in a cellular milieu (153–155). With new technologies, in particular computational tools employing artificial intelligence (156), being developed at a rapid pace, we anticipate that within the next decade, our understanding of eukaryotic ribosome assembly will undergo yet another transformation.

DISCLOSURE STATEMENT

The authors are not aware of any affiliations, memberships, funding, or financial holdings that might be perceived as affecting the objectivity of this review.

ACKNOWLEDGMENTS

We thank all members of the Klinge lab for helpful discussions and comments on the manuscript. Our experimental research on ribosome assembly was supported by the National Institutes of Health (grants 1R01GM145950 and 1R01GM143181) and the G. Harold and Leila Y. Mathers Foundation (grant MF-2104-01554). A.V.B. was supported by a European Molecular Biology Organization long-term fellowship (ALTF 711-2019) and by funds from a Pels Family Center Postdoctoral Fellowship at The Rockefeller University.

LITERATURE CITED

1. Noller HF. 2012. Evolution of protein synthesis from an RNA world. *Cold Spring Harb. Perspect. Biol.* 4(4):a003681
2. Palade GE. 1955. A small particulate component of the cytoplasm. *J. Biophys. Biochem. Cytol.* 1(1):59–68
3. Scherrer K, Latham H, Darnell JE. 1963. Demonstration of an unstable RNA and of a precursor to ribosomal RNA in HeLa cells. *PNAS* 49:240–48
4. Scherrer K, Darnell JE. 1962. Sedimentation characteristics of rapidly labelled RNA from HeLa cells. *Biochem. Biophys. Res. Commun.* 7:486–90
5. Miller OL, Beatty BR. 1969. Visualization of nucleolar genes. *Science* 164(3882):955–57
6. Trapman J, Retèl J, Planta RJ. 1975. Ribosomal precursor particles from yeast. *Exp. Cell Res.* 90(1):95–104

7. Venema J, Tollervey D. 1999. Ribosome synthesis in *Saccharomyces cerevisiae*. *Annu. Rev. Genet.* 33:261–311
8. Rigaut G, Shevchenko A, Rutz B, Wilm M, Mann M, Séraphin B. 1999. A generic protein purification method for protein complex characterization and proteome exploration. *Nat. Biotechnol.* 17(10):1030–32
9. Krogan NJ, Peng W-T, Cagney G, Robinson MD, Haw R, et al. 2004. High-definition macromolecular composition of yeast RNA-processing complexes. *Mol. Cell* 13(2):225–39
10. Woolford JL, Baserga SJ. 2013. Ribosome biogenesis in the yeast *Saccharomyces cerevisiae*. *Genetics* 195(3):643–81
11. Ben-Shem A, Jenner L, Yusupova G, Yusupov M. 2010. Crystal structure of the eukaryotic ribosome. *Science* 330(6008):1203–9
12. Rabl J, Leibundgut M, Ataide SF, Haag A, Ban N. 2011. Crystal structure of the eukaryotic 40S ribosomal subunit in complex with initiation factor 1. *Science* 331(6018):730–36
13. Klinge S, Voigts-Hoffmann F, Leibundgut M, Arpagaus S, Ban N. 2011. Crystal structure of the eukaryotic 60S ribosomal subunit in complex with initiation factor 6. *Science* 334(6058):941–48
14. Ben-Shem A, Garreau de Loubresse N, Melnikov S, Jenner L, Yusupova G, Yusupov M. 2011. The structure of the eukaryotic ribosome at 3.0 Å resolution. *Science* 334(6062):1524–29
15. Granneman S, Kudla G, Petfalski E, Tollervey D. 2009. Identification of protein binding sites on U3 snoRNA and pre-rRNA by UV cross-linking and high-throughput analysis of cDNAs. *PNAS* 106(24):9613–18
16. Kühlbrandt W. 2014. The resolution revolution. *Science* 343(6178):1443–44
17. Wu S, Tutuncuoglu B, Yan K, Brown H, Zhang Y, et al. 2016. Diverse roles of assembly factors revealed by structures of late nuclear pre-60S ribosomes. *Nature* 534(7605):133–37
18. Klinge S, Woolford JL. 2019. Ribosome assembly coming into focus. *Nat. Rev. Mol. Cell Biol.* 20(2):116–31
19. Dörner K, Ruggeri C, Zemp I, Kutay U. 2023. Ribosome biogenesis factors—from names to functions. *EMBO J.* 42:e112699
20. Tartakoff AM, Chen L, Raghavachari S, Gitiforooz D, Dhinakaran A, et al. 2021. The nucleolus as a polarized coaxial cable in which the rDNA axis is surrounded by dynamic subunit-specific phases. *Curr. Biol.* 31(12):2507–19.e4
21. Lafontaine DLJ, Riback JA, Bascetin R, Brangwynne CP. 2021. The nucleolus as a multiphase liquid condensate. *Nat. Rev. Mol. Cell Biol.* 22(3):165–82
22. Musacchio A. 2021. On the role of phase separation in the biogenesis of membraneless compartments. *EMBO J.* 41(5):e109952
23. Neyer S, Kunz M, Geiss C, Hantsche M, Hodirnau V-V, et al. 2016. Structure of RNA polymerase I transcribing ribosomal DNA genes. *Nature* 540(7634):607–10
24. Engel C, Gubbey T, Neyer S, Sainsbury S, Oberthuer C, et al. 2017. Structural basis of RNA polymerase I transcription initiation. *Cell* 169(1):120–31.e22
25. Sadian Y, Baudin F, Tafur L, Murciano B, Wetzel R, et al. 2019. Molecular insight into RNA polymerase I promoter recognition and promoter melting. *Nat. Commun.* 10(1):5543
26. Baudin F, Murciano B, Fung HKH, Fromm SA, Mattei S, et al. 2022. Mechanism of RNA polymerase I selection by transcription factor UAF. *Sci. Adv.* 8(16):eabn5725
27. Kos M, Tollervey D. 2010. Yeast pre-rRNA processing and modification occur cotranscriptionally. *Mol. Cell* 37(6):809–20
28. Bohnsack KE, Bohnsack MT. 2019. Uncovering the assembly pathway of human ribosomes and its emerging links to disease. *EMBO J.* 38(13):e100278
29. Udem SA, Warner JR. 1972. Ribosomal RNA synthesis in *Saccharomyces cerevisiae*. *J. Mol. Biol.* 65(2):227–42
30. Sharma S, Lafontaine DLJ. 2015. "View from a bridge": a new perspective on eukaryotic rRNA base modification. *Trends Biochem. Sci.* 40(10):560–75
31. Sloan KE, Warda AS, Sharma S, Entian K-D, Lafontaine DLJ, Bohnsack MT. 2017. Tuning the ribosome: the influence of rRNA modification on eukaryotic ribosome biogenesis and function. *RNA Biol.* 14(9):1138–52

32. Höbartner C, Bohnsack KE, Bohnsack MT. 2024. How natural enzymes and synthetic ribozymes generate methylated nucleotides in RNA. *Annu. Rev. Biochem.* 93:109–37
33. Lan P, Zhou B, Tan M, Li S, Cao M, et al. 2020. Structural insight into precursor ribosomal RNA processing by ribonuclease MRP. *Science* 369(6504):656–63
34. Schneider C, Bohnsack KE. 2022. Caught in the act—visualizing ribonucleases during eukaryotic ribosome assembly. *WIREs RNA* 14(4):e1766
35. Pillon MC, Gordon J, Frazier MN, Stanley RE. 2021. HEPN RNases—an emerging class of functionally distinct RNA processing and degradation enzymes. *Crit. Rev. Biochem. Mol. Biol.* 56(1):88–108
36. Martin R, Straub AU, Doebele C, Bohnsack MT. 2013. DExD/H-box RNA helicases in ribosome biogenesis. *RNA Biol.* 10(1):4–18
37. Rodríguez-Galán O, García-Gómez JJ, de la Cruz J. 2013. Yeast and human RNA helicases involved in ribosome biogenesis: current status and perspectives. *Biochim. Biophys. Acta Gene Regul. Mech.* 1829(8):775–90
38. Mitterer V, Pertschy B. 2022. RNA folding and functions of RNA helicases in ribosome biogenesis. *RNA Biol.* 19(1):781–810
39. Khreiss A, Bohnsack KE, Bohnsack MT. 2023. Molecular functions of RNA helicases during ribosomal subunit assembly. *Biol. Chem.* 404(8–9):781–89
40. Prattes M, Lo Y-H, Bergler H, Stanley RE. 2019. Shaping the nascent ribosome: AAA-ATPases in eukaryotic ribosome biogenesis. *Biomolecules* 9(11):715
41. Pillet B, Méndez-Godoy A, Murat G, Favre S, Stumpe M, et al. 2022. Dedicated chaperones coordinate co-translational regulation of ribosomal protein production with ribosome assembly to preserve proteostasis. *eLife* 11:e74255
42. Rössler I, Embacher J, Pillet B, Murat G, Liesinger L, et al. 2019. Tsr4 and Nap1, two novel members of the ribosomal protein chaperOME. *Nucleic Acids Res.* 47(13):6984–7002
43. Black JJ, Musalgaonkar S, Johnson AW. 2019. Tsr4 is a cytoplasmic chaperone for the ribosomal protein Rps2 in *Saccharomyces cerevisiae*. *Mol. Cell. Biol.* 39(17):e00094-19
44. Pillet B, Mitterer V, Kressler D, Pertschy B. 2017. Hold on to your friends: dedicated chaperones of ribosomal proteins. *BioEssays* 39(1):e201600153
45. Mougey EB, Pape LK, Sollner-Webb B. 1993. A U3 small nuclear ribonucleoprotein-requiring processing event in the 5′ external transcribed spacer of *Xenopus* precursor rRNA. *Mol. Cell. Biol.* 13(10):5990–98
46. Mougey EB, O'Reilly M, Osheim Y, Miller OL, Beyer A, Sollner-Webb B. 1993. The terminal balls characteristic of eukaryotic rRNA transcription units in chromatin spreads are rRNA processing complexes. *Genes Dev.* 7(8):1609–19
47. Dragon F, Gallagher JEG, Compagnone-Post PA, Mitchell BM, Porwancher KA, et al. 2002. A large nucleolar U3 ribonucleoprotein required for 18S ribosomal RNA biogenesis. *Nature* 417(6892):967–70
48. Grandi P, Rybin V, Bassler J, Petfalski E, Strauss D, et al. 2002. 90S pre-ribosomes include the 35S pre-rRNA, the U3 snoRNP, and 40S subunit processing factors but predominantly lack 60S synthesis factors. *Mol. Cell* 10(1):105–15
49. Tschochner H, Hurt E. 2003. Pre-ribosomes on the road from the nucleolus to the cytoplasm. *Trends Cell Biol.* 13(5):255–63
50. Kornprobst M, Turk M, Kellner N, Cheng J, Flemming D, et al. 2016. Architecture of the 90S preribosome: a structural view on the birth of the eukaryotic ribosome. *Cell* 166(2):380–93
51. Chaker-Margot M, Barandun J, Hunziker M, Klinge S. 2017. Architecture of the yeast small subunit processome. *Science* 355(6321):eaal1880
52. Sun Q, Zhu X, Qi J, An W, Lan P, et al. 2017. Molecular architecture of the 90S small subunit preribosome. *eLife* 6:e22086
53. Cheng J, Kellner N, Berninghausen O, Hurt E, Beckmann R. 2017. 3.2-Å-resolution structure of the 90S preribosome before A1 pre-rRNA cleavage. *Nat. Struct. Mol. Biol.* 24(11):954–64
54. Barandun J, Chaker-Margot M, Hunziker M, Molloy KR, Chait BT, Klinge S. 2017. The complete structure of the small-subunit processome. *Nat. Struct. Mol. Biol.* 24(11):944–53
55. Cheng J, Lau B, Venuta GL, Ameismeier M, Berninghausen O, et al. 2020. 90S pre-ribosome transformation into the primordial 40S subunit. *Science* 369(6510):1470–76

56. Du Y, An W, Zhu X, Sun Q, Qi J, Ye K. 2020. Cryo-EM structure of 90S small ribosomal subunit precursors in transition states. *Science* 369(6510):1477–81
57. Singh S, Vanden Broeck A, Miller L, Chaker-Margot M, Klinge S. 2021. Nucleolar maturation of the human small subunit processome. *Science* 373(6560):eabj5338
58. Krogan NJ, Cagney G, Yu H, Zhong G, Guo X, et al. 2006. Global landscape of protein complexes in the yeast *Saccharomyces cerevisiae*. *Nature* 440(7084):637–43
59. Dosil M, Bustelo XR. 2004. Functional characterization of Pwp2, a WD family protein essential for the assembly of the 90 S pre-ribosomal particle. *J. Biol. Chem.* 279(36):37385–97
60. Pöll G, Li S, Ohmayer U, Hierlmeier T, Milkereit P, Perez-Fernandez J. 2014. In vitro reconstitution of yeast tUTP/UTP A and UTP B subcomplexes provides new insights into their modular architecture. *PLOS ONE* 9(12):e114898
61. Hunziker M, Barandun J, Petfalski E, Tan D, Delan-Forino C, et al. 2016. UtpA and UtpB chaperone nascent pre-ribosomal RNA and U3 snoRNA to initiate eukaryotic ribosome assembly. *Nat. Commun.* 7:12090
62. Pérez-Fernández J, Román A, Rivas JDL, Bustelo XR, Dosil M. 2007. The 90S preribosome is a multimodular structure that is assembled through a hierarchical mechanism. *Mol. Cell. Biol.* 27(15):5414–29
63. Pérez-Fernández J, Martín-Marcos P, Dosil M. 2011. Elucidation of the assembly events required for the recruitment of Utp20, Imp4 and Bms1 onto nascent pre-ribosomes. *Nucleic Acids Res.* 39(18):8105–21
64. Chen J, Zhang L, Ye K. 2020. Functional regions in the 5′ external transcribed spacer of yeast pre-rRNA. *RNA* 26(7):866–77
65. Chaker-Margot M, Hunziker M, Barandun J, Dill BD, Klinge S. 2015. Stage-specific assembly events of the 6-MDa small-subunit processome initiate eukaryotic ribosome biogenesis. *Nat. Struct. Mol. Biol.* 22(11):920–23
66. Zhang L, Wu C, Cai G, Chen S, Ye K. 2016. Stepwise and dynamic assembly of the earliest precursors of small ribosomal subunits in yeast. *Genes Dev.* 30(6):718–32
67. Hunziker M, Barandun J, Buzovetsky O, Steckler C, Molina H, Klinge S. 2019. Conformational switches control early maturation of the eukaryotic small ribosomal subunit. *eLife* 8:213
68. Tomecki R, Labno A, Drazkowska K, Cysewski D, Dziembowski A. 2015. hUTP24 is essential for processing of the human rRNA precursor at site A1, but not at site A0. *RNA Biol.* 12(9):1010–29
69. Wells GR, Weichmann F, Colvin D, Sloan KE, Kudla G, et al. 2016. The PIN domain endonuclease Utp24 cleaves pre-ribosomal RNA at two coupled sites in yeast and humans. *Nucleic Acids Res.* 44(11):5399–409
70. Lau B, Cheng J, Flemming D, Venuta GL, Berninghausen O, et al. 2021. Structure of the maturing 90S pre-ribosome in association with the RNA exosome. *Mol. Cell* 81(2):293–303.e4
71. Thoms M, Thomson E, Bassler J, Gnädig M, Griesel S, Hurt E. 2015. The exosome is recruited to RNA substrates through specific adaptor proteins. *Cell* 162(5):1029–38
72. Vanden Broeck A, Klinge S. 2022. An emerging mechanism for the maturation of the small subunit processome. *Curr. Opin. Struct. Biol.* 73:102331
73. Roychowdhury A, Joret C, Bourgeois G, Heurgué-Hamard V, Lafontaine DLJ, Graille M. 2019. The DEAH-box RNA helicase Dhr1 contains a remarkable carboxyl terminal domain essential for small ribosomal subunit biogenesis. *Nucleic Acids Res.* 47(14):7548–63
74. Boneberg FM, Brandmann T, Kobel L, van den Heuvel J, Bargsten K, et al. 2019. Molecular mechanism of the RNA helicase DHX37 and its activation by UTP14A in ribosome biogenesis. *RNA* 25(6):685–701
75. Sardana R, Liu X, Granneman S, Zhu J, Gill M, et al. 2015. The DEAH-box helicase Dhr1 dissociates U3 from the pre-rRNA to promote formation of the central pseudoknot. *PLOS Biol.* 13(2):e1002083
76. Choudhury P, Hackert P, Memet I, Sloan KE, Bohnsack MT. 2018. The human RNA helicase DHX37 is required for release of the U3 snoRNP from pre-ribosomal particles. *RNA Biol.* 16(1):54–68
77. Cheng J, Venuta GL, Lau B, Berninghausen O, Beckmann R, Hurt E. 2022. In vitro structural maturation of an early stage pre-40S particle coupled with U3 snoRNA release and central pseudoknot formation. *Nucleic Acids Res.* 50(20):11916–23
78. Black JJ, Sardana R, Elmir EW, Johnson AW. 2020. Bud23 promotes the final disassembly of the small subunit processome in *Saccharomyces cerevisiae*. *PLOS Genet.* 16(12):e1009215

79. Ameismeier M, Cheng J, Berninghausen O, Beckmann R. 2018. Visualizing late states of human 40S ribosomal subunit maturation. *Nature* 558(7709):249–53
80. Ameismeier M, Zemp I, van den Heuvel J, Thoms M, Berninghausen O, et al. 2020. Structural basis for the final steps of human 40S ribosome maturation. *Nature* 587(7835):683–87
81. Plassart L, Shayan R, Montellese C, Rinaldi D, Larburu N, et al. 2021. The final step of 40S ribosomal subunit maturation is controlled by a dual key lock. *eLife* 10:e61254
82. Cheng J, Lau B, Thoms M, Ameismeier M, Berninghausen O, et al. 2022. The nucleoplasmic phase of pre-40S formation prior to nuclear export. *Nucleic Acids Res.* 50(20):11924–37
83. Mitterer V, Shayan R, Ferreira-Cerca S, Murat G, Enne T, et al. 2019. Conformational proofreading of distant 40S ribosomal subunit maturation events by a long-range communication mechanism. *Nat. Commun.* 10(1):2754
84. Chen W, Xie Z, Yang F, Ye K. 2017. Stepwise assembly of the earliest precursors of large ribosomal subunits in yeast. *Nucleic Acids Res.* 45(11):6837–47
85. Chaker-Margot M, Klinge S. 2019. Assembly and early maturation of large subunit precursors. *RNA* 25(4):465–71
86. Sanghai ZA, Piwowarczyk R, Vanden Broeck A, Klinge S. 2023. A co-transcriptional ribosome assembly checkpoint controls nascent large ribosomal subunit maturation. *Nat. Struct. Mol. Biol.* 30:594–99
87. Joret C, Capeyrou R, Belhabich-Baumas K, Plisson-Chastang C, Ghandour R, et al. 2018. The Npa1p complex chaperones the assembly of the earliest eukaryotic large ribosomal subunit precursor. *PLOS Genet.* 14(8):e1007597
88. Bhutada P, Favre S, Jaafar M, Hafner J, Liesinger L, et al. 2022. Rbp95 binds to 25S rRNA helix H95 and cooperates with the Npa1 complex during early pre-60S particle maturation. *Nucleic Acids Res.* 50(17):10053–77
89. Ismail S, Flemming D, Thoms M, Gomes-Filho JV, Randau L, et al. 2022. Emergence of the primordial pre-60S from the 90S pre-ribosome. *Cell Rep.* 39(1):110640
90. Bohnsack KE, Henras AK, Nielsen H, Bohnsack MT. 2023. Making ends meet: a universal driver of large ribosomal subunit biogenesis. *Trends Biochem. Sci.* 48(3):213–15
91. Aquino GRR, Hackert P, Krogh N, Pan K-T, Jaafar M, et al. 2021. The RNA helicase Dbp7 promotes domain V/VI compaction and stabilization of inter-domain interactions during early 60S assembly. *Nat. Commun.* 12(1):6152
92. Jaafar M, Contreras J, Dominique C, Martín-Villanueva S, Capeyrou R, et al. 2021. Association of snR190 snoRNA chaperone with early pre-60S particles is regulated by the RNA helicase Dbp7 in yeast. *Nat. Commun.* 12(1):6153
93. Khreiss A, Capeyrou R, Lebaron S, Albert B, Bohnsack KE, et al. 2023. The DEAD-box protein Dbp6 is an ATPase and RNA annealase interacting with the peptidyl transferase center (PTC) of the ribosome. *Nucleic Acids Res.* 51(2):744–64
94. Sanghai ZA, Miller L, Molloy KR, Barandun J, Hunziker M, et al. 2018. Modular assembly of the nucleolar pre-60S ribosomal subunit. *Nature* 556(7699):126–29
95. Kater L, Thoms M, Barrio-Garcia C, Cheng J, Ismail S, et al. 2017. Visualizing the assembly pathway of nucleolar pre-60S ribosomes. *Cell* 171(7):1599–610.e14
96. Zhou D, Zhu X, Zheng S, Tan D, Dong M-Q, Ye K. 2018. Cryo-EM structure of an early precursor of large ribosomal subunit reveals a half-assembled intermediate. *Protein Cell* 10:120–30
97. Liang X, Zuo M-Q, Zhang Y, Li N, Ma C, et al. 2020. Structural snapshots of human pre-60S ribosomal particles before and after nuclear export. *Nat. Commun.* 11(1):3542
98. Kater L, Mitterer V, Thoms M, Cheng J, Berninghausen O, et al. 2020. Construction of the central protuberance and L1 stalk during 60S subunit biogenesis. *Mol. Cell* 79(4):615–28.e5
99. Cruz VE, Sekulski K, Peddada N, Sailer C, Balasubramanian S, et al. 2022. Sequence-specific remodeling of a topologically complex RNP substrate by Spb4. *Nat. Struct. Mol. Biol.* 29(12):1228–38
100. Sekulski K, Cruz VE, Weirich CS, Erzberger JP. 2023. rRNA methylation by Spb1 regulates the GTPase activity of Nog2 during 60S ribosomal subunit assembly. *Nat. Commun.* 14(1):1207
101. Yelland JN, Bravo JPK, Black JJ, Taylor DW, Johnson AW. 2023. A single 2′-*O*-methylation of ribosomal RNA gates assembly of a functional ribosome. *Nat. Struct. Mol. Biol.* 30(1):91–98

102. Prattes M, Grishkovskaya I, Hodirnau V-V, Hetzmannseder C, Zisser G, et al. 2022. Visualizing maturation factor extraction from the nascent ribosome by the AAA-ATPase Drg1. *Nat. Struct. Mol. Biol.* 29(9):942–53
103. Li Z, Chen S, Zhao L, Huang G, Xu H, et al. 2023. Nuclear export of pre-60S particles through the nuclear pore complex. *Nature* 618(7964):411–18
104. Lau B, Huang Z, Kellner N, Niu S, Berninghausen O, et al. 2023. Mechanism of 5S RNP recruitment and helicase-surveilled rRNA maturation during pre-60S biogenesis. *EMBO Rep*. 24:e56910
105. Mitterer V, Thoms M, Buschauer R, Berninghausen O, Hurt E, Beckmann R. 2023. Concurrent remodelling of nucleolar 60S subunit precursors by the Rea1 ATPase and Spb4 RNA helicase. *eLife* 12:e84877
106. Vanden Broeck A, Klinge S. 2023. Principles of human pre-60S biogenesis. *Science* 381(6653):eadh3892
107. Pratte D, Singh U, Murat G, Kressler D. 2013. Mak5 and Ebp2 act together on early pre-60S particles and their reduced functionality bypasses the requirement for the essential pre-60S factor Nsa1. *PLOS ONE* 8(12):e82741
108. Lo Y-H, Sobhany M, Hsu AL, Ford BL, Krahn JM, et al. 2019. Cryo-EM structure of the essential ribosome assembly AAA-ATPase Rix7. *Nat. Commun*. 10(1):513
109. Kocaman S, Lo Y-H, Krahn JM, Sobhany M, Dandey VP, et al. 2022. Communication network within the essential AAA-ATPase Rix7 drives ribosome assembly. *PNAS Nexus* 1(4):pgac118
110. Brüning L, Hackert P, Martin R, Gallesio JD, Aquino GRR, et al. 2018. RNA helicases mediate structural transitions and compositional changes in pre-ribosomal complexes. *Nat. Commun.* 9(1):5383
111. Gerhardy S, Oborská-Oplová M, Gillet L, Börner R, van Nues R, et al. 2021. Puf6 primes 60S preribosome nuclear export at low temperature. *Nat. Commun.* 12(1):4696
112. Chen Z, Suzuki H, Kobayashi Y, Wang AC, DiMaio F, et al. 2018. Structural insights into Mdn1, an essential AAA protein required for ribosome biogenesis. *Cell* 175(3):822–34.e18
113. Sosnowski P, Urnavicius L, Boland A, Fagiewicz R, Busselez J, et al. 2018. The cryoEM structure of the *Saccharomyces cerevisiae* ribosome maturation factor Rea1. *eLife* 7:e39163
114. Gordon J, Chapus FL, Viverette EG, Williams JG, Deterding LJ, et al. 2022. Cryo-EM reveals the architecture of the PELP1-WDR18 molecular scaffold. *Nat. Commun.* 13(1):6783
115. Micic J, Li Y, Wu S, Wilson D, Tutuncuoglu B, et al. 2020. Coupling of 5S RNP rotation with maturation of functional centers during large ribosomal subunit assembly. *Nat. Commun.* 11(1):3751
116. Mickolajczyk KJ, Olinares PDB, Niu Y, Chen N, Warrington SE, et al. 2020. Long-range intramolecular allostery and regulation in the dynein-like AAA protein Mdn1. *PNAS* 117(31):18459–69
117. Thoms M, Mitterer V, Kater L, Falquet L, Beckmann R, et al. 2018. Suppressor mutations in Rpf2–Rrs1 or Rpl5 bypass the Cgr1 function for pre-ribosomal 5S RNP-rotation. *Nat. Commun.* 9(1):4094
118. Moy TI, Boettner D, Rhodes JC, Silver PA, Askew DS. 2002. Identification of a role for *Saccharomyces cerevisiae* Cgr1p in pre-rRNA processing and 60S ribosome subunit synthesis. *Microbiology* 148(4):1081–90
119. Cepeda LPP, Bagatelli FFM, Santos RM, Santos MDM, Nogueira FCS, Oliveira CC. 2019. The ribosome assembly factor Nop53 controls association of the RNA exosome with pre-60S particles in yeast. *J. Biol. Chem.* 294(50):19365–80
120. Galani K, Nissan TA, Petfalski E, Tollervey D, Hurt E. 2004. Rea1, a dynein-related nuclear AAA-ATPase, is involved in late rRNA processing and nuclear export of 60 S subunits. *J. Biol. Chem.* 279(53):55411–18
121. Gordon J, Pillon MC, Stanley RE. 2019. Nol9 is a spatial regulator for the human ITS2 pre-rRNA endonuclease-kinase complex. *J. Mol. Biol.* 431(19):3771–86
122. Fromm L, Falk S, Flemming D, Schuller JM, Thoms M, et al. 2017. Reconstitution of the complete pathway of ITS2 processing at the pre-ribosome. *Nat. Commun.* 8(1):1787
123. Schuller JM, Falk S, Fromm L, Hurt E, Conti E. 2018. Structure of the nuclear exosome captured on a maturing preribosome. *Science* 360(6385):219–22
124. Zhou Y, Musalgaonkar S, Johnson AW, Taylor DW. 2019. Tightly-orchestrated rearrangements govern catalytic center assembly of the ribosome. *Nat. Commun.* 10(1):958
125. Kargas V, Castro-Hartmann P, Escudero-Urquijo N, Dent K, Hilcenko C, et al. 2019. Mechanism of completion of peptidyltransferase centre assembly in eukaryotes. *eLife* 8:213

126. Musalgaonkar S, Black JJ, Johnson AW. 2019. The L1 stalk is required for efficient export of nascent large ribosomal subunits in yeast. *RNA* 25(11):1549–60
127. Sarkar A, Thoms M, Barrio-Garcia C, Thomson E, Flemming D, et al. 2017. Preribosomes escaping from the nucleus are caught during translation by cytoplasmic quality control. *Nat. Struct. Mol. Biol.* 24(12):1107–15
128. Biedka S, Micic J, Wilson D, Brown H, Diorio-Toth L, Woolford JL. 2018. Hierarchical recruitment of ribosomal proteins and assembly factors remodels nucleolar pre-60S ribosomes. *J. Cell Biol.* 248:jcb.201711037
129. Prattes M, Grishkovskaya I, Hodirnau V-V, Rössler I, Klein I, et al. 2021. Structural basis for inhibition of the AAA-ATPase Drg1 by diazaborine. *Nat. Commun.* 12(1):3483
130. Ma C, Wu D, Chen Q, Gao N. 2022. Structural dynamics of AAA + ATPase Drg1 and mechanism of benzo-diazaborine inhibition. *Nat. Commun.* 13(1):6765
131. Nicolas E, Parisot P, Pinto-Monteiro C, de Walque R, Vleeschouwer CD, Lafontaine DLJ. 2016. Involvement of human ribosomal proteins in nucleolar structure and p53-dependent nucleolar stress. *Nat. Commun.* 7:11390
132. Yao R-W, Xu G, Wang Y, Shan L, Luan P-F, et al. 2019. Nascent pre-rRNA sorting via phase separation drives the assembly of dense fibrillar components in the human nucleolus. *Mol. Cell* 76(5):767–83
133. Shan L, Xu G, Yao R-W, Luan P-F, Huang Y, et al. 2023. Nucleolar URB1 ensures 3′ ETS rRNA removal to prevent exosome surveillance. *Nature* 615(7952):526–34
134. Pelava A, Schneider C, Watkins NJ. 2016. The importance of ribosome production, and the 5S RNP–MDM2 pathway, in health and disease. *Biochem. Soc. Trans.* 44(4):1086–90
135. Khajuria RK, Munschauer M, Ulirsch JC, Fiorini C, Ludwig LS, et al. 2018. Ribosome levels selectively regulate translation and lineage commitment in human hematopoiesis. *Cell* 173(1):90–103.e19
136. Mills EW, Green R. 2017. Ribosomopathies: There's strength in numbers. *Science* 358(6363):eaan2755
137. Farley-Barnes KI, Ogawa LM, Baserga SJ. 2019. Ribosomopathies: old concepts, new controversies. *Trends Genet.* 35(10):754–67
138. Ulirsch JC, Verboon JM, Kazerounian S, Guo MH, Yuan D, et al. 2019. The genetic landscape of Diamond-Blackfan anemia. *Am. J. Hum. Genet.* 103(6):930–47. Correction. 2019. *Am. J. Hum. Genet.* 104(2):356
139. Lezzerini M, Penzo M, O'Donohue M-F, dos Santos Vieira CM, Saby M, et al. 2020. Ribosomal protein gene RPL9 variants can differentially impair ribosome function and cellular metabolism. *Nucleic Acids Res.* 48(2):770–87
140. Lebaron S, O'Donohue M, Smith SC, Engleman KL, Juusola J, et al. 2022. Functionally impaired RPL8 variants associated with Diamond-Blackfan anemia and a Diamond-Blackfan anemia-like phenotype. *Hum. Mutat.* 43(3):389–402
141. O'Donohue M-F, Costa LD, Lezzerini M, Unal S, Joret C, et al. 2022. HEATR3 variants impair nuclear import of uL18 (RPL5) and drive Diamond-Blackfan anemia. *Blood* 139(21):3111–26
142. Hannan KM, Soo P, Wong MS, Lee JK, Hein N, et al. 2022. Nuclear stabilization of p53 requires a functional nucleolar surveillance pathway. *Cell Rep.* 41(5):111571
143. Robertson N, Shchepachev V, Wright D, Turowski TW, Spanos C, et al. 2022. A disease-linked lncRNA mutation in RNase MRP inhibits ribosome synthesis. *Nat. Commun.* 13(1):649
144. Nieto B, Gaspar SG, Moriggi G, Pestov DG, Bustelo XR, Dosil M. 2020. Identification of distinct maturation steps involved in human 40S ribosomal subunit biosynthesis. *Nat. Commun.* 11(1):156
145. Nieto B, Gaspar SG, Sapio RT, Clavaín L, Bustelo XR, et al. 2021. Efficient fractionation and analysis of ribosome assembly intermediates in human cells. *RNA Biol.* 18(Suppl. 1):182–97
146. Pellegrino S, Dent KC, Spikes T, Warren AJ. 2023. Cryo-EM reconstruction of the human 40S ribosomal subunit at 2.15 Å resolution. *Nucleic Acids Res.* 51(8):4043–54
147. Faille A, Dent KC, Pellegrino S, Jaako P, Warren AJ. 2023. The chemical landscape of the human ribosome at 1.67 Å resolution. bioRxiv 2023.02.28.530191. **https://doi.org/10.1101/2023.02.28.530191**
148. Holm M, Natchiar SK, Rundlet EJ, Myasnikov AG, Watson ZL, et al. 2023. mRNA decoding in human is kinetically and structurally distinct from bacteria. *Nature* 617(7959):200–7

149. Rodgers ML, Woodson SA. 2021. A roadmap for rRNA folding and assembly during transcription. *Trends Biochem. Sci.* 46(11):889–901
150. Gor K, Duss O. 2023. Emerging quantitative biochemical, structural, and biophysical methods for studying ribosome and protein–RNA complex assembly. *Biomolecules* 13(5):866
151. Han X-R, Sasaki N, Jackson SC, Wang P, Li Z, et al. 2020. $CRL4^{DCAF1/VprBP}$ E3 ubiquitin ligase controls ribosome biogenesis, cell proliferation, and development. *Sci. Adv.* 6(51):eabd6078
152. Dörner K, Badertscher L, Horváth B, Hollandi R, Molnár C, et al. 2022. Genome-wide RNAi screen identifies novel players in human 60S subunit biogenesis including key enzymes of polyamine metabolism. *Nucleic Acids Res.* 50(5):2872–88
153. Erdmann PS, Hou Z, Klumpe S, Khavnekar S, Beck F, et al. 2021. In situ cryo-electron tomography reveals gradient organization of ribosome biogenesis in intact nucleoli. *Nat. Commun.* 12(1):5364–69
154. Lucas BA, Zhang K, Loerch S, Grigorieff N. 2022. In situ single particle classification reveals distinct 60S maturation intermediates in cells. *eLife* 11:e79272
155. Xing H, Taniguchi R, Khusainov I, Kreysing JP, Welsch S, et al. 2023. Translation dynamics in human cells visualized at high resolution reveal cancer drug action. *Science* 381(6653):70–75
156. Jumper J, Evans R, Pritzel A, Green T, Figurnov M, et al. 2021. Highly accurate protein structure prediction with AlphaFold. *Nature* 596(7873):583–89